Numerical Analysis of Trap-Induced Negative Capacitance in Organic Light-Emitting Diodes

V. Georgakopoulos-Paltidis*,**, E. Stanzani*, S. Jenatsch*, D. Braga*, B. Blülle* ,B. Ruhstaller*,***

****Fluxim AG, Winterthur, Switzerland***

*****University of Bayreuth, School of Mathematics and Natural Sciences, Bayreuth, Bavaria, Germany***

******Zürich University of Applied Sciences, Institute of Computational Physics, Winterthur, Switzerland***

Abstract

Impedance spectroscopy (IS) is widely used to study trap dynamics in Organic Light-Emitting Diodes (OLEDs).
Here, we demonstrate how to identify charge-trapping at bulk defects in OLEDs via careful analyses of the device's impedance spectra. Our drift-diffusion simulations go beyond simple mechanistic descriptions, such as equivalent-circuit modelling. We highlight how the dynamic carrier capture and release process can express itself as a strong positive or negative capacitance, depending on the detailed trap interaction.
We performed drift-diffusion simulations to understand the impedance response of a reference polymer LED, i.e., a single-layer device with the PPV-based copolymer super yellow (SY). SY PLEDs have been shown to possess negative capacitance at low frequencies and exhibit considerable charge trapping. Overall, we explained why the C-V characteristics of OLEDs often show negative capacitance and provided a better understanding of the effects of traps in OLEDs. Our robust analysis, based on drift-diffusion simulations, can help understand performance degradations due to trap generations during OLED operations.

Author Keywords

Organic light-emitting diodes; Negative capacitance; Drift-diffusion simulations; Impedance spectroscopy; Charge transport; Device degradation; Defect analysis.

1. Introduction

Organic light-emitting diodes (OLEDs) are an attractive technology for displays and lighting applications due to their mechanical flexibility, solution-processability, and potential for low-cost fabrication (1). In a single-layer polymer light-emitting diode (PLED), an electroluminescent conjugated polymer is sandwiched between two electrodes, enabling electron and hole injection that recombine radiatively within the polymer layer. The stability and efficiency of such a device are influenced by intrinsic factors, related to the materials in the stack and their interfaces, and extrinsic like high operational temperatures and humidity. In this respect, it is well known that charge-trapping states play a dominant role by severely degrading the device's performance (2). Traps can arise from impurities, defects in the polymer backbone, or by-products formed during device operation (e.g., side reactions with oxygen or moisture. These localized states can capture charge carriers, reducing their mobility and disrupting the balance of electron-hole recombination. Over time, this leads to the increase of non-radiative decay pathways, reduced luminous efficiency, and, eventually, device failure (3). A detailed understanding of the molecular processes that create, fill, and deactivate these trap states is crucial for designing more stable polymers, optimizing device architectures, and extending the operational lifetime of PLEDs.

Impedance spectroscopy (IS) is particularly useful for studying trap states in semiconductors and semiconducting devices (4). The response of a material to an applied alternating current (AC) signal is measured over a range of frequencies. Researchers can obtain insights into charge transport, dielectric relaxation, and interfacial phenomena at play through the frequency-dependent behaviour of impedance, comprising real (resistive) and imaginary (reactive) components (5). Generally, the impedance response is analyzed by using equivalent circuit (EC) models. In the case of a material with traps, an EC module would incorporate additional elements to represent defect-related processes (e.g., extra RC elements for trap levels), make it possible to extract trap density, energy distribution, and capture/emission rates (6). However, it is often difficult to attribute a unique equivalent circuit to a specific impedance response. Here we show how to go beyond the simple mechanistic EC descriptions of a PLED impedance response by using drift-diffusion simulations. Our results highlight the role of charge balance, trap depth, and trap site density in determining the low-frequency capacitive behaviour of single-layer OLEDs. A commonly occurring phenomenon that is observed especially in PLEDs is negative capacitance (NC) at low frequencies, which has been explained via injection through interfacial states (7) and charge trapping (8). We establish conditions under which negative capacitance (NC) appears, correlating it with deep trap levels and slow capture-release dynamics. This approach offers insights into charge transport and creates opportunities for alternative degradation modeling strategies for OLED.

2. Physical models

Several models are employed to perform a complete OLED operation simulation during an impedance experiment. The basic drift-diffusion model consists of continuity and the Poisson equations 1-4.

$$\frac{\partial n}{\partial t} = \frac{\nabla J_n}{-q} - R_{n,p}^{Langevin} - R_{nt}^{SRH} \quad (1)$$

$$\frac{\partial p}{\partial t} = \frac{\nabla J_p}{-q} - R_{n,p}^{Langevin} - R_{pt}^{SRH} \quad (2)$$

$$\frac{\partial n_t}{\partial t} = C_n\, n\,(N_t - n_t) - e_n\, n_t + e_p\,(N_t - n_t) - C_p\, p\, n_t \quad (3)$$

$$\nabla(\varepsilon\varepsilon_0 E) = q(p - n - n_t) \quad (4)$$

Langevin and Shockley Reed Hall (SRH) theory is used to describe the recombination processes between free and trapped carriers.

$$R_{n,p}^{Langevin} = \eta\,(\mu_n + \mu_p)\,\frac{q}{\varepsilon}\,(np - n_i^2) \quad (5)$$

$$R_{nt}^{SRH} = C_n\, n\, (N_t - n_t) - e_n\, n_t \quad (6)$$

$$e_n = C_n N_{0,N} \exp\left(\frac{E_t - LUMO}{k_B T}\right) \quad (7)$$

The equations are solved in a coupled scheme to get the steady-state solution for a specific applied bias voltage. The explanation for all symbols can be found in Table 1. The impedance calculation is performed using small signal analysis (SSA), a method that uses the steady-state solution, adding a small AC signal $V(t) = V_0 + V_{amp} sin(\omega t)$ where V_0 is the offset voltage, V_{amp} is the voltage amplitude, and ω is the angular frequency $2\pi f$. If the voltage amplitude V_{amp} is small enough, the system can be considered as linear and, therefore, the current density j(t) is also sinusoidal. The method has been described in previous publications (9) and is implemented in the commercial software Setfos (10).

Table 1

Symbol	Explanation	Units
(n, p, n_t)	Electron, Hole, Trap density	m−3
$(J_{n,p})$	Electron, Hole current density	A·m−2
(q)	Elementary charge	C
(ε)	Relative permittivity	
(ε_0)	Vacuum permittivity	F m−1
(E)	Electric field	V·m−1
(η)	Langevin reduction factor	
$(\mu_{n,p})$	Electron, hole mobility	m2 V−1 s−1
(n_i)	Intrinsic carrier density	m−3
(k_B)	Boltzmann constant	J K−1
(T)	Absolute temperature	K
$(R_{n,p}^{Langevin})$	Langevin recombination rate	m−3 s−1
$(R_{nt,pt}^{SRH})$	SRH recombination rate	m−3 s−1
$(C_{n,p})$	Electron., Hole capture coefficient	m3 s−1
(N_t)	Total trap site concentration	m−3
$(N_{0,N})$	Density of states	m−3
(E_t)	Trap energy level	J
(LUMO)	Lowest Unoccupied Molecular Orbital energy	J
$(e_{n,p})$	Electron, Hole emission rate from trap level	s−1

3. Simulations

We performed drift-diffusion simulations to understand the impedance response of a reference PLED, i.e., a single-layer device with the PPV-based copolymer super yellow (SY). SY PLEDs have been shown to possess NC at low frequencies and exhibit considerable charge-trapping (11).

Our analysis considers three different cases at different charge injection regimes:

a) 0 eV electron and 0.3 eV hole injection barrier. High electron injection, or "N-type majority".

b) 0.3 eV electron and 0 eV hole injection barrier. High hole injection, or "P-type majority".

c) 0.2 eV electron and 0.2 eV hole injection barrier. Equal electron-hole injection, or "Balanced".

For the rest of the paper, plots designated with the letters a,b, and c correspond to simulations of PLEDs in the above different regimes.

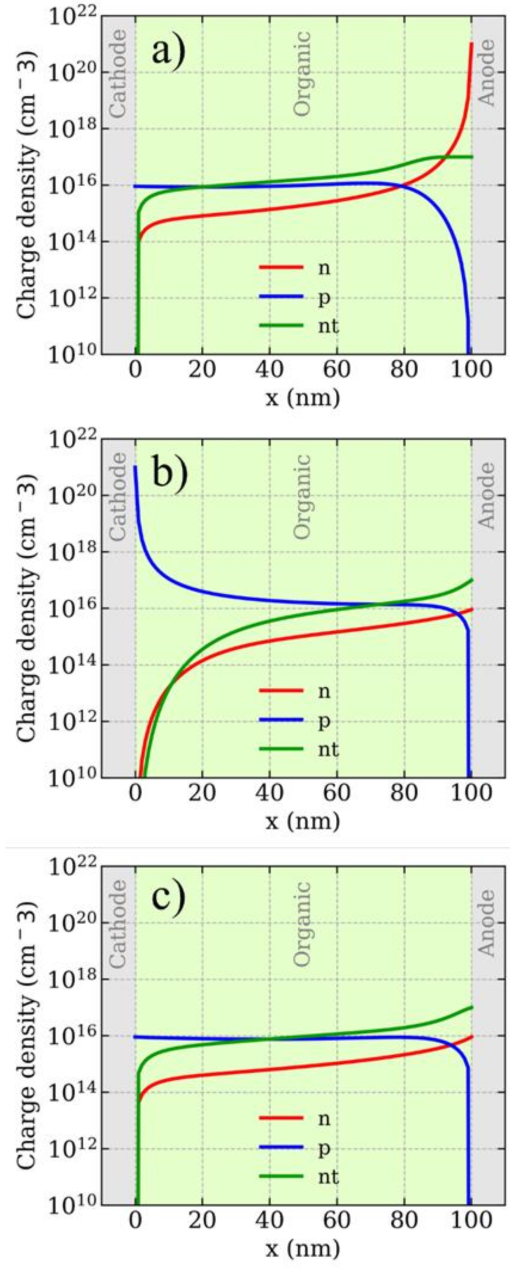

Figure 1 (a-c). Electron (n), hole (p) and trapped electron (nt) density profiles across the active layer in our SY-PLEDs.

4. Results

Figure 1 (a-c) showcases the charge density profiles developed under the distinct charge injection regimes. Different plots correspond to simulated SY-PLEDs with different positions of the electrode Fermi levels. A uniform electron trap site density $N_t = 10^{17} cm^{-3}$ and an energetic depth of $E_t = 0.5\ eV$ is considered while the forward bias voltage is pinned at 2.5V. Clearly, an efficient electron injection (scenario a)) is crucial in the presence of trap states, as the electron current of PPV derivatives has been shown to have an inverse relationship to trap density N_t in PPV.

We simulated the capacitance-voltage (C-V) spectra in the low-frequency limit by varying the energetic depth of the traps and the trap density. Figure 2 (a-c) shows the simulated characteristics of our PLEDs with trap energy E_t from 0.1 to 0.6 eV while assuming slow capture rates $C_{n,p} = 10^{-13}\text{cm}^3\, s^{-1}$ and fixed density of trap sites $N_t = 10^{17}$ (12).

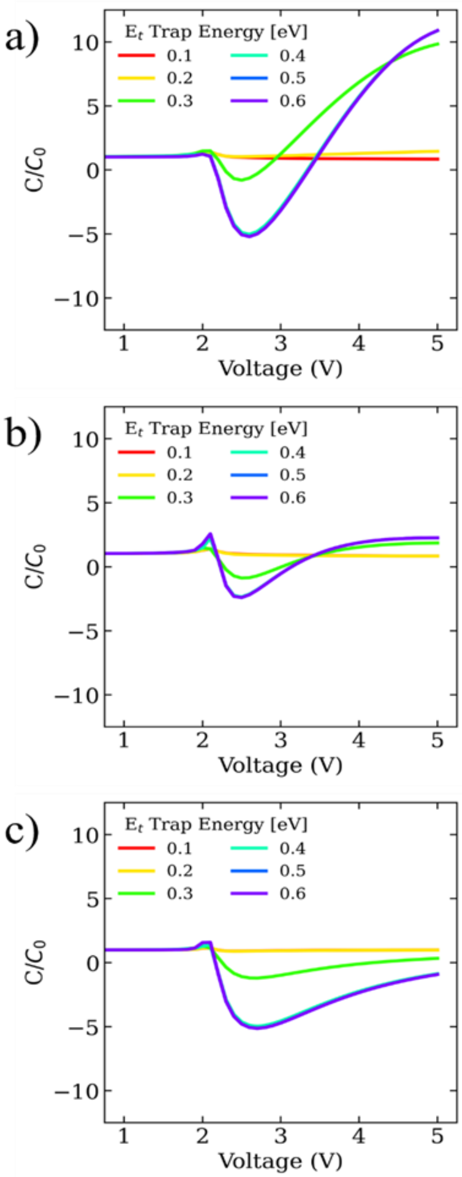

Figure 2. Capacitance as a function of voltage in the low-frequency limit at different trap energetic depths. The trap density is fixed at $N_t = 10^{17} cm^{-3}$.

We identify distinct regions of interest. Below 1V, the capacitance is close to its geometric value C_0 as the device is not conductive in this regime. At voltages from ~ 1.5V to 2V, the capacitance increases, and the device current is dominated by SRH recombination as the traps are not yet filled ($nt \gg n$). The capacitance rises because charges are redistributing inside the active layer in response to the filling of the electron traps that are now capturing holes from the conduction band, hence the increase in non-radiative recombination. At higher voltages, when the traps are filled, the current is driven mainly by Langevin recombination. The capacitance decreases and, eventually, becomes negative when the trap depth is higher than 0.2 eV.

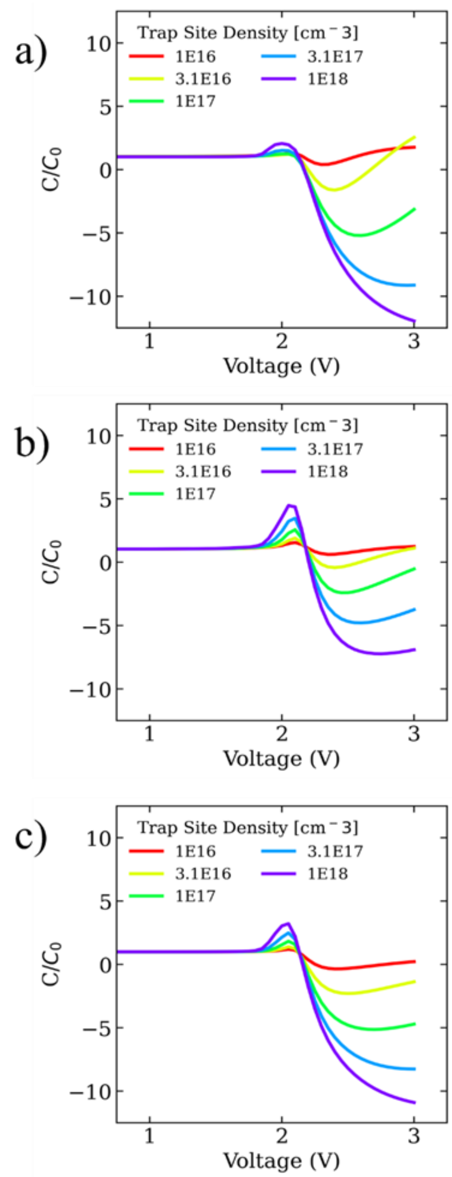

Figure 3. Capacitance as a function of voltage in the low-frequency limit at different trap densities. The trap energetic depth is fixed at E_t= 0.5 eV.

The interaction between the free carriers and the static charge is influenced by the charge balance, capturing coefficients and the trap energy level. On the other hand, we notice that the negative capacitance is a universal property irrespective of the charge balance, which distinguishes the CV characteristics of our PLEDS for trap levels $E_t > 0.2\ eV$ at forward bias and with similar peak intensity for a range of E_t: $0.3 - 0.6\ eV$. Figure 3 (a-c) shows the C-V characteristics of a PLED with E_t= 0.5 eV and different trap densities. Also here, it is clear that at high enough voltages, NC is always present in the case of deep charge trapping. This suggests that negative capacitance could serve as a reliable indicator of the presence of deep trap states. An increase in N_t yields a monotonic increase in the magnitude of NC. The relationship between NC and N_t provides a clear signal of defect growth, which could be used, for example, during accelerated lifetime analyses instead of further complex separated experiments.

5. Discussion

In literature, efforts have been made to understand the origin of negative capacitance and how to use this to determine the density of trap sites in a material. In bipolar organic diodes, biomolecular recombination was proposed as the mechanism responsible for NC (13). The diode was assumed to operate in an SRH-dominated regime, and this allowed the authors to estimate the trap density in these simple devices. On the other hand, a complete description that would allow this feature to be used for the analysis of OLEDs is not available. The approach proposed by Niu *et al.* doesn't apply to PLEDs, where both Langevin (radiative) and SRH (non-radiative) recombination coexist in the forward bias regime. A more generalized approach is needed because when Langevin and SRH recombination coexist, the analytical solutions require simplification of the equations that aren't always entirely justified. In our simulation, we see indeed a mixture of Langevin and SRH recombination as contributing factors, and achieving an analytical solution to the equation is, therefore, impossible. Further analyses are required to separate these two contributions and use the NC as a tool to analyse traps in OLEDs. The answer to which the recombination mechanism is dominating lies in the relative strength of the capture coefficients and Langevin recombination, together with the influence of the biomolecular recombination perfectors (14).

In conclusion, our study demonstrates the influence of charge balance trap depth and trap site density on the low-frequency forward bias capacitive features of a single-layer organic layer OLED featuring negative capacitance. The investigation yielded specific parameters for the appearance of NC as well as predicted evolution of this measurement under defect-generating current stress, paving the way for a more comprehensive degradation modeling. Our robust analysis can help understand performance degradations due to trap generations during OLED operations.

6. Acknowledgements

This project has been partly funded by the European Union Horizon 2021 research and innovation program under grant agreement No. 101073045 (TADF*solutions*)

7. References

1. Friend RH, Gymer RW, Holmes AB, Burroughes JH, Marks RN, Taliani C, et al. Electroluminescence in conjugated polymers. 1999;397.
2. Abbaszadeh D, Kunz A, Kotadiya NB, Mondal A, Andrienko D, Michels JJ, et al. Electron Trapping in Conjugated Polymers. Chem Mater. 2019 Sep 10;31(17):6380–6.
3. Scholz S, Kondakov D, Lüssem B, Leo K. Degradation Mechanisms and Reactions in Organic Light-Emitting Devices. Chem Rev. 2015 Aug 26;115(16):8449–503.
4. Nguyen TP, Renaud C, Huang CH, Lo CN, Lee CW, Hsu CS. Effect of electrical operation on the defect states in organic semiconductors. J Mater Sci: Mater Electron. 2008 Dec;19(S1):92–5.
5. Takada M, Nagase T, Kobayashi T, Naito H. Full characterization of electronic transport properties in working polymer light-emitting diodes via impedance spectroscopy. Journal of Applied Physics. 2019 Mar 21;125(11):115501.
6. Djidjou TK, Basel T, Rogachev A. Admittance spectroscopy study of polymer diodes in small magnetic fields. Journal of Applied Physics. 2012 Jul 15;112(2):024511.
7. Bisquert J, Garcia-Belmonte G, Pitarch Á, Bolink HJ. Negative capacitance caused by electron injection through interfacial states in organic light-emitting diodes. Chemical Physics Letters. 2006 Apr;422(1–3):184–91.
8. Ehrenfreund E, Lungenschmied C, Dennler G, Neugebauer H, Sariciftci NS. Negative capacitance in organic semiconductor devices: Bipolar injection and charge recombination mechanism. Applied Physics Letters. 2007 Jul 2;91(1):012112.
9. Jenatsch S, Züfle S, Blülle B, Ruhstaller B. Combining steady-state with frequency and time domain data to quantitatively analyze charge transport in organic light-emitting diodes. Journal of Applied Physics. 2020 Jan 21;127(3):031102.
10. Fluxim AG, Switzerland, see www.fluxim.com for Simulation software Setfos.
11. Diethelm M, Penninck L, Regnat M, Offermans T, Zimmermann B, Kirsch C, et al. Finite element modeling for analysis of electroluminescence and infrared images of thin-film solar cells. Solar Energy. 2020 Oct;209:186–93.
12. Diethelm M, Bauer M, Hu W, Vael C, Jenatsch S, Blom PWM, et al. Electron Trap Dynamics in Polymer Light-Emitting Diodes. Adv Funct Materials. 2022 Jul;32(27):2106185.
13. Niu Q, Crăciun NI, Wetzelaer GJAH, Blom PWM. Origin of Negative Capacitance in Bipolar Organic Diodes. Phys Rev Lett. 2018 Mar 14;120(11):116602.
14. Lakhwani G, Rao A, Friend RH. Bimolecular Recombination in Organic Photovoltaics. Annu Rev Phys Chem. 2014 Apr 1;65(1):557–81.